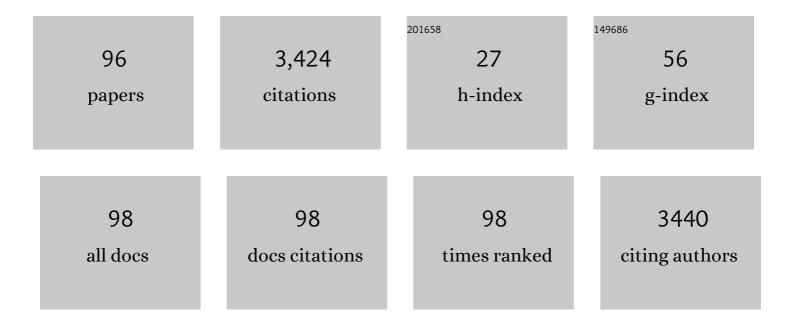
Michael G Tanner

List of Publications by Year in descending order

Source: https://exaly.com/author-pdf/1164222/publications.pdf Version: 2024-02-01



#	Article	IF	CITATIONS
1	Selective Plane Illumination Fluorescence Endomicroscopy using a Polymer Imaging Fiber and an End-cap. , 2022, , .		Ο
2	Molecular detection of Gram-positive bacteria in the human lung through an optical fiber–based endoscope. European Journal of Nuclear Medicine and Molecular Imaging, 2021, 48, 800-807.	6.4	14
3	Ultrafast laser ablation of a multicore polymer optical fiber for multipoint light emission. Optics Express, 2021, 29, 20765.	3.4	6
4	A hydrogel-based optical fibre fluorescent pH sensor for observing lung tumor tissue acidity. Analytica Chimica Acta, 2020, 1134, 136-143.	5.4	38
5	Time-Resolved Spectroscopy of Fluorescence Quenching in Optical Fibre-Based pH Sensors. Sensors, 2020, 20, 6115.	3.8	8
6	Observing mode-dependent wavelength-to-time mapping in few-mode fibers using a single-photon detector array. APL Photonics, 2020, 5, .	5.7	12
7	Frugal filtering optical lenses for point-of-care diagnostics. Biomedical Optics Express, 2020, 11, 1864.	2.9	6
8	Ultrafast-laser-ablation-assisted spatially selective attachment of fluorescent sensors onto optical fibers. Optics Letters, 2020, 45, 2716.	3.3	5
9	Core crosstalk in ordered imaging fiber bundles. Optics Letters, 2020, 45, 6490.	3.3	10
10	10.1063/5.0006983.1. , 2020, , .		0
11	Fibre-based ratiometric fluorescence imaging for contrast enhancement of spectrally similar signals in the lung. , 2020, , .		1
12	High fidelity fibre-based physiological sensing deep in tissue. Scientific Reports, 2019, 9, 7713.	3.3	10
13	Endoscopic sensing of distal lung physiology. Journal of Physics: Conference Series, 2019, 1151, 012009.	0.4	0
14	Polymer Microarrays for the Discovery and Optimization of Robust Optical-Fiber-Based pH Sensors. ACS Combinatorial Science, 2019, 21, 417-424.	3.8	15
15	Developing Novel Fibres for Endoscopic Imaging and Sensing. , 2019, , .		Ο
16	Ultraâ€low background Raman sensing using a negativeâ€curvature fibre and no distal optics. Journal of Biophotonics, 2019, 12, e201800239.	2.3	15
17	High-speed dual color fluorescence lifetime endomicroscopy for highly-multiplexed pulmonary diagnostic applications and detection of labeled bacteria. Biomedical Optics Express, 2019, 10, 181.	2.9	13
18	Fibre-based spectral ratio endomicroscopy for contrast enhancement of bacterial imaging and pulmonary autofluorescence. Biomedical Optics Express, 2019, 10, 1856.	2.9	15

#	Article	IF	CITATIONS
19	Characterising cross-coupling in coherent fibre bundles. , 2019, , .		2
20	Discovery of a robust optical fibre pH sensor based using polymer microarrays. , 2019, , .		0
21	Dual purpose fibre – SERS pH sensing and bacterial analysis. Analyst, The, 2018, 143, 5918-5925.	3.5	7
22	Ultra-low Background Raman Sensing Using a Negative-curvature Fibre. , 2018, , .		0
23	A multifunctional endoscope for imaging, fluid delivery and fluid extraction (Conference) Tj ETQq1 1 0.784314 rg	gBT /Overl	oc <u>k</u> 10 Tf 5
24	Multispectral fibre endoscope imaging system for enhanced visualisation of smartprobes (Conference) Tj ETQq0	0 0 rgBT /	Overlock 10
25	Early arriving photon imaging for locating optical endomicroscopy fibres and medical devices (Conference Presentation). , 2018, , .		0
26	Time-resolved single photon spectroscopy through a single optical fibre for miniaturised medical probe design. , 2018, , .		0
27	Chip-based quantum key distribution. Nature Communications, 2017, 8, 13984.	12.8	232
28	Endoscopic sensing of pH in the distal lung (Conference Presentation). , 2017, , .		0
29	Fibre optic time-resolved spectroscopy using CMOS-SPAD arrays. Proceedings of SPIE, 2017, , .	0.8	7
30	Controlled core-to-core photo-polymerisation – fabrication of an optical fibre-based pH sensor. Analyst, The, 2017, 142, 3569-3572.	3.5	13
31	Multiplexed fibre optic sensing in the distal lung (Conference Presentation). , 2017, , .		1
32	Silicon photonic processor of two-qubit entangling quantum logic. Journal of Optics (United) Tj ETQq0 0 0 rgBT /	Overlock	10 Tf 50 222
33	Endoscopic sensing of alveolar pH. Biomedical Optics Express, 2017, 8, 243.	2.9	31
34	Ballistic and snake photon imaging for locating optical endomicroscopy fibres. Biomedical Optics Express, 2017, 8, 4077.	2.9	19
35	Time-resolved spectroscopy at 19,000 lines per second using a CMOS SPAD line array enables advanced biophotonics applications. Optics Express, 2017, 25, 11103.	3.4	32

Characterization and modelling of inter-core coupling in coherent fiber bundles. Optics Express, 2017, 25, 11932. 3.4 24

#	Article	IF	CITATIONS
37	pH sensing through a single optical fibre using SERS and CMOS SPAD line arrays. Optics Express, 2017, 25, 30976.	3.4	25
38	High-extinction ratio integrated photonic filters for silicon quantum photonics. Optics Letters, 2017, 42, 815.	3.3	72
39	A tunable fiber-coupled optical cavity for agile enhancement of detector absorption. Journal of Applied Physics, 2016, 120, .	2.5	3
40	Resonance fluorescence from a telecom-wavelength quantum dot. Applied Physics Letters, 2016, 109, .	3.3	17
41	Two-color widefield fluorescence microendoscopy enables multiplexed molecular imaging in the alveolar space of human lung tissue. Journal of Biomedical Optics, 2016, 21, 1.	2.6	33
42	Photon-sparse microscopy: Trans-wavelength ghost imaging. Proceedings of SPIE, 2016, , .	0.8	0
43	Chip-to-chip quantum photonic interconnect by path-polarization interconversion. Optica, 2016, 3, 407.	9.3	108
44	Comparison of Photon Pair Generation in a-Si:H and c-Si Microring Resonators. , 2016, , .		0
45	Ground state solver on a silicon quantum photonic chip. , 2016, , .		0
46	Passive High-Extinction Integrated Photonic Filters for Silicon Quantum Photonics. , 2016, , .		1
47	Bayesian quantum phase estimation on an integrated Silicon photonic device. , 2016, , .		0
48	Photon-sparse microscopy: visible light imaging using infrared illumination. Optica, 2015, 2, 1049.	9.3	109
49	Integrated Photonic Devices for Quantum Key Distribution. , 2015, , .		0
50	Chip-to-chip quantum entanglement distribution. , 2015, , .		1
51	Nanoantenna Enhancement for Telecom-Wavelength Superconducting Single Photon Detectors. Nano Letters, 2015, 15, 819-822.	9.1	28
52	Two-photon interference at telecom wavelengths for time-bin-encoded single photons from quantum-dot spin qubits. Nature Communications, 2015, 6, 8955.	12.8	31
53	Background-free Quantum Frequency Downconversion for Two-photon Interference of Heterogeneous Photon Sources. , 2015, , .		0
54	Photonic qubit entanglement and processing in silicon waveguides. , 2015, , .		3

4

#	Article	lF	CITATIONS
55	Trans-spectral Ghost Microscopy. , 2015, , .		Ο
56	Entanglement distribution between integrated silicon photonic chips. , 2015, , .		0
57	Optimised quantum hacking of superconducting nanowire single-photon detectors. Optics Express, 2014, 22, 6734.	3.4	39
58	Gallium arsenide (GaAs) quantum photonic waveguide circuits. Optics Communications, 2014, 327, 49-55.	2.1	98
59	Nano-optical observation of cascade switching in a parallel superconducting nanowire single photon detector. Applied Physics Letters, 2014, 104, .	3.3	12
60	On-chip quantum interference between silicon photon-pair sources. Nature Photonics, 2014, 8, 104-108.	31.4	407
61	Parallel superconducting strip-line detectors: reset behaviour in the single-strip switch regime. Superconductor Science and Technology, 2014, 27, 044029.	3.5	6
62	Infrared photon counting with superconducting nanowire single-photon detectors. , 2013, , .		0
63	Current distribution in a parallel configuration superconducting strip-line detector. Applied Physics Letters, 2013, 103, .	3.3	14
64	Singlet oxygen luminescence detection with a fibre-coupled superconducting nanowire single-photon detector. , 2013, , .		0
65	Nano-optical measurements of novel superconducting single photon detector designs. , 2013, , .		0
66	Kilometer-range, high resolution depth imaging via 1560 nm wavelength single-photon detection. Optics Express, 2013, 21, 8904.	3.4	239
67	Photon pair generation in a silicon micro-ring resonator with reverse bias enhancement. Optics Express, 2013, 21, 27826.	3.4	137
68	Kilometre-range, high resolution depth imaging using 1560 nm wavelength single-photon detection. , 2013, , .		0
69	Singlet oxygen luminescence detection with a fiber-coupled superconducting nanowire single-photon detector. Optics Express, 2013, 21, 5005.	3.4	125
70	Singlet Oxygen luminescence detection with a fiber-coupled superconducting nanowire single-photon detector. , 2013, , .		1
71	Analysis of a distributed fiber-optic temperature sensor using single-photon detectors. Optics Express, 2012, 20, 3456.	3.4	41

72 Silicon Quantum Photonic Sources and Circuits. , 2012, , .

#	Article	IF	CITATIONS
73	Superconducting nanowire single-photon detectors: physics and applications. Superconductor Science and Technology, 2012, 25, 063001.	3.5	731
74	Depth imaging at kilometer range using time-correlated single-photon counting at wavelengths of 850 nm and 1560 nm. , 2012, , .		2
75	A superconducting nanowire single photon detector on lithium niobate. Nanotechnology, 2012, 23, 505201.	2.6	38
76	Quantum interference and manipulation of entanglement in silicon wire waveguide quantum circuits. New Journal of Physics, 2012, 14, 045003.	2.9	71
77	Fast Path and Polarization Manipulation of Telecom Wavelength Single Photons in Lithium Niobate Waveguide Devices. Physical Review Letters, 2012, 108, 053601.	7.8	87
78	Quantum interference in silicon waveguide circuits. , 2011, , .		2
79	An Analysis of Single-Photon Detectors in an Environmentally Robust GigaHertz Clock Rate Quantum Key Distribution System. , 2011, , .		Ο
80	Correlated photon-pair generation in a periodically poled MgO doped stoichiometric lithium tantalate reverse proton exchanged waveguide. Applied Physics Letters, 2011, 99, .	3.3	27
81	Single-photon counting imaging systems. , 2011, , .		Ο
82	Generation of correlated photon pairs in a chalcogenide As2S3 waveguide. Applied Physics Letters, 2011, 98, .	3.3	62
83	Spatial dependence of output pulse delay in a niobium nitride nanowire superconducting single-photon detector. Applied Physics Letters, 2011, 98, 201116.	3.3	34
84	High-resolution single-mode fiber-optic distributed Raman sensor for absolute temperature measurement using superconducting nanowire single-photon detectors. Applied Physics Letters, 2011, 99, .	3.3	82
85	Analysis of detector performance in a gigahertz clock rate quantum key distribution system. New Journal of Physics, 2011, 13, 075008.	2.9	27
86	Detection of charge motion in a non-metallic silicon isolated double quantum dot. New Journal of Physics, 2011, 13, 103012.	2.9	11
87	Kilometer range depth imaging using time-correlated single-photon counting. , 2011, , .		1
88	Generation of Correlated Photons in an Integrated Chalcogenide As_2S_3 Waveguide. , 2011, , .		0
89	High Spatial Resolution Distributed Fiber Sensor Using Raman Scattering in Single-Mode Fiber. , 2010, , .		2
90	Enhanced telecom wavelength single-photon detection with NbTiN superconducting nanowires on oxidized silicon. Applied Physics Letters, 2010, 96, .	3.3	99

#	Article	IF	CITATIONS
91	Nano-Optical Studies of Superconducting Nanowire Single Photon Detectors. Lecture Notes of the Institute for Computer Sciences, Social-Informatics and Telecommunications Engineering, 2010, , 158-166.	0.3	0
92	Indirect observation of periodic charge polarization in silicon isolated double quantum dots. Journal of Applied Physics, 2009, 106, 043713.	2.5	2
93	Fine and Large Coulomb Diamonds in a Silicon Quantum Dot. Japanese Journal of Applied Physics, 2009, 48, 06FF15.	1.5	18
94	Controlled polarisation and excitation of silicon on insulator isolated double quantum dots with remote charge sensing. , 2008, , .		0
95	Investigation of silicon isolated double quantum-dot energy levels for quantum computation. Microelectronic Engineering, 2006, 83, 1818-1822.	2.4	9
96	Geometry dependence of the energy levels in silicon isolated double quantum-dots. Microelectronic Engineering, 2005, 78-79, 195-200.	2.4	2